Engineering towards catalytic use of fungal class-II peroxidases for dye-decolorizing and conversion of lignin model compounds

Lundell, Taina Kristina

2017

Lundell , T K , Bentley , E , Hilden , S K , Rytioja , J T , Kuuskeri , J T , Ufot , U F , Nousiainen , P A , Hofrichter , M , Wahlsten , M P-V , Doyle , W & Smith , A T 2017 , ' Engineering towards catalytic use of fungal class-II peroxidases for dye-decolorizing and conversion of lignin model compounds ' , Current Biotechnology , vol. 6 , no. 2 , pp. 116-117 . https://doi.org/10.2174/2211550105666160520120101

http://hdl.handle.net/10138/307256
https://doi.org/10.2174/2211550105666160520120101

acceptedVersion

Special issue in Current Biotechnology on "Fungal Biotechnology"

ENGINEERING TOWARDS CATALYTIC USE OF FUNGAL CLASS-II PEROXIDASES FOR DYE-DECOLORIZING AND CONVERSION OF LIGNIN MODEL COMPOUNDS

Taina Lundell[1*], Elodie Bentley[2⁺], Kristiina Hildén[1], Johanna Rytioja[1], Jaana Kuuskeri[1], Usenobong F. Ufot[2], Paula Nousiainen[3], Martin Hofrichter[4], Matti Wahlsten[1], Wendy Doyle[2], Andrew T. Smith[5]

[1]*Microbiology and Biotechnology, Department of Food and Environmental Sciences, University of Helsinki, Finland*

[2]*Department of Chemistry and Biochemistry, School of Life Sciences, University of Sussex, United Kingdom*

[3]*Department of Chemistry, Laboratory of Organic Chemistry, University of Helsinki, Finland*

[4]*IHI Zittau, Technical University of Dresden, Germany*

[5]*School of Applied Sciences, RMIT University, Melbourne, Australia*

[⁺]*In memoriam*

***Correspondence to:** Taina Lundell, Microbiology and Biotechnology, Department of Food and Environmental Sciences, P.O. Box 56, Viikki Biocenter 1, FI-00014 University of Helsinki, Finland. Tel: +358294159316. Email: taina.lundell@helsinki.fi

Abstract

Background. Manganese peroxidases (MnP) and lignin peroxidases (LiP) are haem-including fungal secreted class-II peroxidases, which are interesting oxidoreductases in protein engineering aimed at design of biocatalysts for lignin and lignocellulose conversion, dye compound degradation, activation of aromatic compounds, and biofuel production.

Objective. Recombinant short-type MnP (Pr-MnP3) of the white rot fungus *Phlebia radiata*, and its manganese-binding site (E40, E44, D186) directed variants were produced and characterized. To allow catalytic applications, enzymatic bleaching of Reactive Blue 5 and conversion of lignin-like compounds by engineered class-II peroxidases were explored.

Method. Pr-MnP3 and its variants were expressed in *Escherichia coli*. The resultant body proteins were lysed, purified and refolded into haem-including enzymes in 6-7% protein recovery, and examined spectroscopically and kinetically.

Results. Successful production of active enzymes was attained, with spectral characteristics of high-spin class-II peroxidases. Recombinant Pr-MnP3 demonstrated high affinity to Mn^{2+}, which was noticeably affected by single (D186H/N) and double (E40H+E44H) mutations. Without addition of Mn^{2+}, Pr-MnP3 was able to oxidize ABTS and decolorize Reactive Blue 5. Pc-LiPH8, its Trp-radical site variants, and engineered CiP-LiP demonstrated conversion of veratryl alcohol and dimeric non-phenolic lignin-model compounds (arylglycerol-β-aryl ethers) with production of veratraldehyde, which is evidence for cation radical formation with subsequent C_α-C_β cleavage. Pc-LiPH8 and CiP variants were able to effectively oxidize and convert the phenolic dimer (guaiacylglycerol-β–guaiacyl ether).

Conclusion. Our results demonstrate suitability of engineered MnP and LiP peroxidases for dye-decolorizing, and efficiency of LiP and its variants for activation and degradation of phenolic and non-phenolic lignin-like aryl ether-linked compounds.

Running title: Engineered fungal class-II peroxidases for conversion of lignin compounds

Key words: manganese peroxidase, lignin peroxidase, white-rot fungi, lignin biodegradation, dye decolorizing, *Phlebia radiata*, recombinant enzyme, protein engineering

INTRODUCTION

Fungal class-II peroxidases are haem-including, secreted oxidoreductase enzymes belonging to the large haem peroxidase superfamily previously named as “plant peroxidase superfamily”, nowadays known as “non-animal peroxidases” or “plant-peroxidase like superfamily” [1,2]. This superfamily is comprised of haem-containing proteins of conserved secondary structure and globin-like fold with peroxidase (H_2O_2 -> 2 H_2O) oxidoreductive activity, and was initially divided to three classes: class-I prokaryotic-like organelle peroxidases (such as cytochrome-*c* peroxidase), class-II fungal secreted peroxidases, and class-III plant secreted peroxidases (such as horseradish peroxidase) [3]. The class-II peroxidases are represented in fungi in multigene families, especially in species of the Basidiomycota fungal class Agaricomycotina, which includes the so called white-rot fungi that are capable of complete dissection of plant lignocelluloses including conversion and degradation of the lignin moieties [4–6].

Furthermore, the fungal class-II haem-peroxidases are divided into several subfamilies according to their protein structures and catalytic activities [1,7,8]. The subfamilies encompass a variety of the lignin-modifying, high-redox potential substrate compound attacking enzymes, namely lignin peroxidases (LiP, EC 1.11.1.14), short and long-type manganese peroxidases (MnP, EC 1.11.1.13) and versatile peroxidases (VP, EC 1.11.1.16) [4-10]. In addition to the high-redox potential peroxidases, Basidiomycota fungi may possess atypical and “low-redox potential” class-II peroxidases – one of them is the classic *Coprinus (Coprinopsis) cinerea* peroxidase CiP [1,5-8,10-11].

LiP and MnP enzymes were at first described in the white-rot fungus *Phanerochaete chrysosporium* [12,13], and thereafter in several other wood-decaying polypore species [6,10,14]. In most of the saprotrophic wood lignin-degrading and litter-decomposing Agaricomycetes species, a general pattern of multigene enzyme families of short-type of MnPs, including also atypical-short-MnPs, VPs and atypical-VPs are identified together with a few genes codifying generic low-redox potential class-II peroxidases [4-6]. On the contrary, LiPs and long-MnPs are more restricted to the wood-decaying and lignin-attacking Polyporales species [4].

LiP is an efficient oxidoreductase with ability to oxidize even high-redox potential and lignin-subunit mimicking, non-phenolic aromatic substrate molecules like veratryl (3,4-dimethoxybenzyl) alcohol and dimeric aryl-ether linked lignin model compounds, and directly interact with polymeric lignin [1,10,14–16]. The physiological function of MnP is that of oxidation of Mn^{2+} ions to Mn^{3+} ions which are chelated by dicarboxylic acids leading to oxidative depolymerisation of phenolic compounds or activation of lignin substructures [1,7-10,12,13,17,18], and MnP has been shown to depolymerise lignin *in vitro* [19]. Moreover, this enzyme mediates initial steps in the degradation of high-molecular weight lignin [18-21]. VPs in turn share protein and catalytic properties of both LiPs and MnPs [7,8].

Crystal structure of *P. chrysosporium* MnPH4 clearly presents one Mn ion binding site in the vicinity of the second haem propionate within a short channel to the C-terminal surface of the protein [22]. Mn^{2+} is hexacoordinated including the haem propionate and three conserved, acidic amino-acid residues (two Glu and one Asp) forming the Mn^{2+}-binding site. This site as demonstrated by 3D homology modelling is present in the two divergent *Phlebia radiata* enzymes Pr-MnP3 and Pr-MnP2 [9].

The production of recombinant proteins and their variants made by site-directed mutagenesis is a pre-requisite for enzyme structure-function studies. The first active haem peroxidase of the non-animal peroxidase (plant-peroxidase like) superfamily to be over-expressed heterologously in a bacterial host was a class-I type haem peroxidase, the yeast mitochondrial cytochrome-*c* peroxidase (CcP) [23]. Since CcP expression, *Escherichia coli* has been used to express recombinant class-II and class-III peroxidase proteins: *Armoracia*

rusticana (horseradish) peroxidase HRPC [24], *P. chrysosporium* LiPH8 [25], *Pleurotus eryngii* VP [8,26], and long-MnP (MnPH4) from *P. chrysosporium* [27].

This work was aimed at characterization of the short-type MnP3 of *P. radiata*, and generation of alterations in the Mn-binding site by site-directed mutagenesis. We present catalytic abilities of similarly engineered fungal class-II peroxidases with different substrate specificities (LiPs, CiP, CiP-LiP), which were compared for oxidation and conversion of lignin-like model compounds, and for bleaching of the anthraquinone-aniline-derived polymeric dye compound Reactive Blue 5. These results are also indicative of potential applicability of the engineered LiP peroxidases for activation and conversion of aromatic compounds and lignin substructures.

Materials and Methods

2.1 Materials

Chemicals used in this investigation were of reagent grade and obtained from Thermo Fisher Scientific or Sigma-Aldrich Co. as pure commercial products, and were used without further purification, except veratryl alcohol, which was distilled before use. The lignin model compound dimers (Fig. 1) were synthesized at the Department of Chemistry, University of Helsinki, according to the procedure of Nakatsubo et al. [28], including three (β-O-4) type lignin-substructure aromatic compounds, the dimeric arylglycerol-β-aryl ethers [1-(4-hydroxy-3-methoxyphenyl)-2-(2-methoxyphenoxy)-1,3-dihydroxypropane] (**3,** 'Erol'), [1-(3,4-dimethoxyphenyl)-2-(2-methoxyphenoxy)-1,3-dihydroxypropane] (**4,** 'Adlerol'), [1-(3,4-dimethoxyphenyl)-2-(4-methoxyphenoxy)-1,3-dihydroxypropane] (**5,** 'p-Adlerol') (Fig. 1). Veratryl alcohol (**1,** 3,4-dimethoxybenzyl alcohol) and veratraldehyde (**2,** 3,4-dimethoxybenzaldehyde) were purchased from Sigma-Fluka. All restriction enzymes and their appropriate buffers were supplied by New England Biolabs Ltd. *E. coli* cells TOP10 and DH5α (Thermo Fisher Scientific) were applied for cloning, and *E. coli* strain W3110 (ATCC27325) cells for production of recombinant proteins adopting the expression vector pFLAG1 (International Biotechnologies Inc.). Recombinant Pc-LiPH8, its two variants (E250Q,

E250Q+E168Q), synthetic CiP, and engineered CiP-LiP (CiP-D179W+R258E+R272D) were previously produced by using *E. coli* expression and refolding [25,29–31]. Native wild-type class-II peroxidases (Pr-LiP3, Pr-MnP3) were previously produced and purified from cultures of *Phlebia radiata* 79 (FBCC0043) [32,33].

2.2 Structural modelling of Pr-MnP3 protein

The overall folding structure of recombinant Pr-MnP3 enzyme was homology modelled and visualized using RasWin Web Lab Viewer in reference to the crystal structure coordinates of recombinant class-II VP from *Pleurotus eryngii* (RCSB PDB Protein Data Bank structure 3FJW, Piontek K *et al.* 2009). A detailed view to the Pr-MnP3 manganese-binding site was created accordingly (Fig. 2).

2.3 Production of recombinant Pr-MnP3 and its site-directed mutants

Previously cloned and characterized *P. radiata mnp3* (pCR2.1-*Pr-mnp3*) coding region cDNA (NCBI GenBank accession AJ310930) [9] was used as template for recombinant protein expression. To create the *Pr-mnp3* expression cassette, two sets of new primers were designed. The 5’ sense primer MnP3-Nt (5’- GAA TTC CAT ATG TTA ACT GTG GCT TGC CCA GAT GGT GTG AAC ACT GC -3’) included *Eco*RI and *Nde*I restriction sites and additional codons for Met, Leu and Thr to mimic the N-terminus construction of the highly in *E. coli* expressed synthetic CiP and LiP enzymes [30], and the first ten codons in frame of the mature *mnp3* coding sequence. The 3’ antisense primer MnP3-Ct (5′- GAA TTC GGA TCC TTA CGA CGG GGG GAC AGG CGC AAC AGA -3′) was complementary to the last eight codons of the *mnp3* and *Bam*HI and *Eco*RI restriction sites.

Whole Plasmid Amplification Method (WPAM) PCR using pFLAG1-*mnp3* as template was adopted for site-directed mutagenesis [34,35] with two primer-designed strategies. Five different Mn-binding site variants of Pr-MnP3 were constructed: E40H and E44H mutations and a double mutant (E40H+E44H) by substituting codons of Glu40 and Glu44 with His codons at both positions. For each mutant, a mutagenic and a reverse primer were designed

complementary to opposite strands of the same DNA region. Primers used in site-directed mutagenesis were (mutations underlined) the E40H mutagenic primer 5'- CAC CTC GTG GCC ACA CTC GCC -3'; E40H reverse primer 5 - CAC CTC GCC ACA CTC GCC -3'; E44H mutagenic primer 5'- CAC TCT CTG CGC CTC ACG TTC -3', and E44H reverse primer 5' –CAC CTC GCC ACA CTC GCC -3'. For the double mutant (E40H+E44H), mutagenic and reverse primers were those designed for E40H and E44H. To introduce site-specific D186N and D186H mutations with incorporation of *Pvu*II restriction site, the primers used were (mutations underlined) the D186N mutagenic primer 5'- CTG CCA ATC ACG TCG ACC CAT CGA TCC-3', D186N reverse primer 5'- CTG CGA TCG TGT GCG ACG CGA G -3', D186H mutagenic primer 5'- CTG CCC ATC ACG TCG ACC CAT CGA TCC -3', and D186H reverse primer 5'- CTG CGA TCG TGT GCG ACG CGA G -3'. The mutant DNA fragments were inserted into the pFLAG1 and cloned (*E. coli* DH5α). After complete sequencing of the plasmid inserts, one of the positive clones for wild-type like enzyme and each mutant was used to transform *E. coli* W3110 cells for protein expression.

The following amplification conditions were used: 5 ng of template DNA, 1 mM each dNTP, 10 µM of each primer, 10 units of *Pfu* DNA polymerase (Promega) and 1 X reaction buffer. PCR conditions were as follows: initial denaturation at 95°C for 10 min and 25 cycles of (i) denaturation at 95°C for 1 min, (ii) annealing at 60°C for 1 min, (iii) extension at 72°C for 1 min, and finally at 72°C for 16 min. Annealing temperature was 50°C for site-directed mutagenesis PCR.

2.4 Recombinant protein production, refolding and purification of Pr-MnP3 and variant enzymes

Production of recombinant Pr-MnP3 was performed in 500 ml of Terrific Broth (Sigma-Aldrich) and supplemented with 100 µg/ml ampicillin and induced with 1 mM IPTG as described previously [25,26]. The cells were harvested by centrifugation, and protein pellets were re-suspended and incubated in lysis buffer (50 mM Tris-HCl, pH 8.0), 1 mM EDTA, 30 mM DTT, 10 M urea, and 2 mg/ml of lysozyme). The cells were further disrupted by sonication and centrifuged at 15,000 rpm for 30 min to obtain inclusion bodies containing the recombinant proteins, and the pellet was re-suspended in wash solution (20 mM Tris-

HCl, pH 8.0, 1 mM EDTA, and 5 mM DTT). Membrane components and proteases were removed by washing the pellet three times with the wash solution containing 3 % Triton X-100 and re-centrifuged at 15,000 rpm for 30 minutes. Recombinant Pr-MnP3 proteins were solubilised in 50 mM Tris-HCl buffer (pH 8.0) containing 1 mM EDTA, 1 mM DTT and 6 M urea for 15 min before centrifugation at 15,000 rpm for 30 min to remove the remaining insoluble materials.

Refolding of Pr-MnP3 and its variants into active enzymes was carried out according to the methods adopted for refolding of recombinant HRP, LiPH8, VP and CiP [24-26,31]. The refolding of 200 µg/ml of recombinant Pr-MnP3 was performed in 50 mM Tris-HCl (pH 9.5), 5 mM $CaCl_2$, 0.5 mM glutathione disulphide (GSSG), 0.1 mM DTT, 0.15 M urea and 20 µM haemin containing solution after which proteins were ultrafiltrated under N_2 pressure in an Amicon stirred cell with a 10 kDa pore size membrane (Amicon), and dialysed into 20 mM sodium acetate (pH 4.3) buffer containing 1 mM $CaCl_2$, at +4°C overnight. Proteins in solution were further dialysed into 10 mM sodium succinate (pH 6.0) buffer with 1 mM $CaCl_2$, then loaded into a 50 ml Mono-Q anion exchange column (Pharmacia) and eluted with a linear gradient of NaCl from 0 to 0.5 M in 10 mM sodium succinate (pH 6.0). The fractions with high MnP activity as determined by oxidation of Mn^{2+} (see chapter 2.6), and showing absorbance peak at 408 nm (Soret band maximum for native enzyme) were collected and gel-filtered into 10 mM sodium succinate buffer (pH 6.0) with 0.2 mM $CaCl_2$ using a PD10 desalting column (Pharmacia). The purified protein solution was frozen in liquid nitrogen and stored at -80°C. Molecular size as mass of the recombinant enzyme was determined both in 12 % SDS-PAGE and using MALDI-TOF-MS analysis (Mass Spectrometry Centre, University of Sussex) [35].

2.5 Spectral properties of recombinant Pr-MnP3 and its variants

Resting-state UV-visible absorbance spectra (250-750 nm) of recombinant peroxidases in 10 mM sodium succinate (pH 6.0) were recorded at 25°C using a Shimadzu UV-2401 PC spectrophotometer. Concentration of recombinant Pr-MnP3, Pc-LiPH8, CiP, and their variants were calculated from the absorption at the haem peroxidase Soret band maximum at 408 nm of the resting state spectrum using an extinction coefficient of 168 $mM^{-1}cm^{-1}$ [36]. The Reinheitszahl value (R_Z) was estimated as a ratio of A_{408}/A_{280}. Extinction coefficient

for Pr-MnP3 and its variants was determined by the pyridine haemochrome method and calculated using the extinction coefficient for the reduced – oxidised haem ($A_{555} - A_{542}$) = 20.7 mM $^{-1}cm^{-1}$ [36].

2.6 Steady-state kinetics of recombinant and native Pr-MnP3 enzymes

Steady-state kinetic properties (K_m and k_{cat} values) of the engineered Pr-MnP3 and its Mn-binding site variants were determined using Mn^{2+} ions as the reducing substrate. The reactions were carried out at 25 °C in 100 mM sodium tartrate buffer, pH 5.0, using a range of Mn^{2+} concentrations (20 µM - 1.0 mM) as $MnSO_4$, 8.0 nM to 150 nM of each enzyme, and were initiated by addition of 100 µM H_2O_2. Three parallel reactions were recorded at 238 nm to follow generation of the Mn^{3+}-tartrate complex using ε_{238} = 6500 M^{-1} cm^{-1} [17]. For ABTS as the reducing substrate, 100 mM sodium tartrate buffer, pH 3.0, was used with 10 nM to 6.5 mM of each enzyme, addition of Mn^{2+} was omitted, and individual reactions for each enzyme at 25 °C were followed at 414 nm to detect initial rates of formation of the ABTS radical using ε_{414} = 36.8 $mM^{-1}cm^{-1}$ [37]. All reactions were performed in triplicate, and the mean values with standard deviation are reported. MS Excel software was used for data collection and calculations.

Steady-state kinetics and affinity to various reducing substrates was also determined for the wild-type native enzyme Pr-MnP3, which was purified from *P. radiata* culture fluids [33,38], by using a Shimadzu UV-1700 spectrophotometer. Oxidation of Mn^{2+} as $MnSO_4$ in 10 mM sodium malonate buffer (pH 4.5) was determined at 25 °C as chelates at 270 nm [17]. Various aromatic compound reducing substrates (phenols and amines) were tested for the native enzyme in order to determine potential Mn-independent oxidation activity, similar to the ABTS assays omitting addition of Mn^{2+} ions, and to allow comparison to VP and general peroxidase activities [1,7,8,39].

2.7 Decolorizing (bleaching) of Reactive Blue 5

Catalytic efficiency of recombinant *E. coli* expressed class-II peroxidases were tested for bleaching of the anthraquinone-derivative polymeric phenylamine (aniline) textile dye

compound Reactive Blue 5 (RB5) as substrate (Fig. 1). Bleaching of RB5 is a specific character for the fungal secreted, haem-including dye-decolorizing peroxidase DyP [40], which belongs to another haem-peroxidase superfamily divergent from the class-II peroxidases [1]. Enzyme reactions were performed in 96-well plastic microplates using 165 µl reaction volume, 10 mM sodium malonate buffer (pH 3.0), 10 µM RB5 and 0.2 µg of each enzyme. Reactions were initiated with addition of 50 µM H_2O_2, and absorbance change at 598 nm was followed for 10-20 min using a Tecan Infinite M300 plate-reader spectrophotometer, at a constant temperature of 25 °C. Three technical replicates for each reaction and enzyme were recorded, and the mean value kinetic traces were produced by using the Tecan Magellan (version 1.0), MS Excel and Origin software.

2.8 Lignin model compound oxidation and degradation

The ability of recombinant class-II peroxidases to act on veratryl alcohol and lignin-substructure like dimeric aromatic compounds (Fig. 1) was tested by performing steady-state kinetic experiments in 1 ml reaction volumes, in 10 mM sodium succinate buffer at pH 3.0, using 1 µl (2-10 nkat) of each enzyme. Concentration of each lignin model compound in the conversion reactions was 0.2 mM, except for Pc-LiPH8, when substrate concentrations of both 0.2 mM and 2.0 mM were used. Reactions were initiated with addition of 100 µM H_2O_2, and increase of absorbance at 310 nm was recorded, at a constant temperature of 25 °C, for 5-10 min using Shimadzu UV-VIS 1700 spectrophotometer. Extinction coefficient 9300 M^{-1} cm^{-1} for formation of veratraldehyde at 310 nm was adopted [32,36].

In addition, the substrate conversion reactions were continued for 1-2 h with gentle mixing every 30 min and addition of 100 µM H_2O_2, then kept overnight at 25 °C, and stopped by freezing at -80 °C. Product compounds were identified and quantified with Agilent 1100 HPLC connected to Zorbax C-18 column (100 mm x 2.1 mm, 5 µm particle size) and diode-array detector. Compound elution was performed with 0.35 ml min^{-1} flow rate at 40 °C by using a gradient of acidic (pH 3.0 adjusted with TFA) water phase (100% - 30%) and acetonitrile (0-70%) within 15 min of run time. HPLC samples (5 µl injection volume) were prepared from thawed reactions by filtering through 0.2 µm pore size membrane devices (Acropac GH, Gelman Sciences). Product quantification and identification was based on

reference compounds, and identification was confirmed by ion trap mass spectrometer (Agilent 1100 Series LC/MSD Trap XCT Plus).

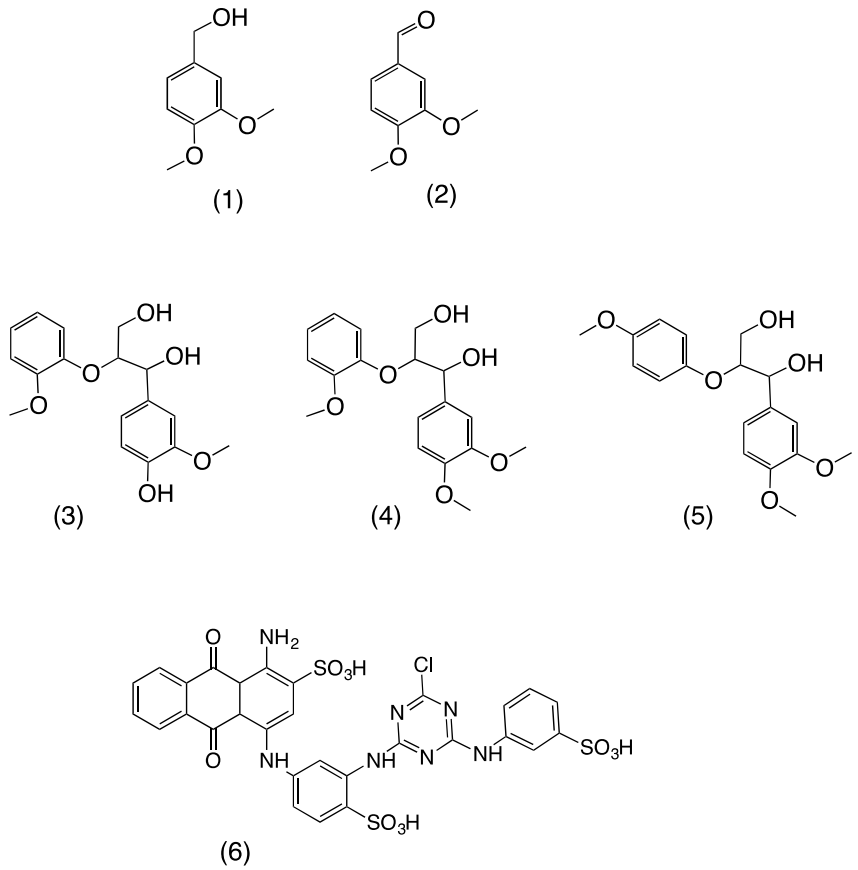

Figure 1. Chemical structures of the substrates used in the peroxidase kinetic and overnight reactions. From the left, lignin-like model compounds: (**1**) veratryl alcohol [(3,4-dimethoxybenzyl) alcohol], (**3**) "erol" dimer [1-(4-hydroxy-3-methoxyphenyl)-2-(2-methoxyphenoxy)-1,3-dihydroxypropane], (**4**) "adlerol" dimer [1-(3,4-dimethoxyphenyl)-2-(2-methoxyphenoxy)-1,3-dihydroxypropane], (**5**) "*p*-adlerol" dimer [1-(3,4-dimethoxyphenyl)-2-(4-methoxyphenoxy)-1,3-dihydroxypropane]. Compound (**2**) veratraldehyde [(3,4-dimethoxybenzaldehyde)] was the main product followed in the oxidations of (**1**), (**4**) and (**5**). Compound (**6**) Reactive Blue 5 was used as a substrate in the dye-decolorizing experiments.

3. RESULTS and DISCUSSION

3.1 Production and structure of recombinant Pr-MnP3

Several native wild-type class-II peroxidases of *Phlebia radiata* have been purified from liquid and lignocellulose cultures [32,33,38,41], and three *lip* and two divergent *mnp* genes

were previously cloned and characterized [9,42]. However, individual enzymes were not yet expressed in recombinant form to allow full enzymatic characterization, or more systematic testing of their catalytic abilities and suitability for bioconversion reactions.

The native Pr-MnP3 enzyme of *P. radiata* is able to act on solid pine wood, and in the presence of unsaturated lipids, malonic acid and Mn^{2+} ions, and constant production of H_2O_2, the reactions result with some release and de-polymerisation of wood aromatic compounds [33]. Thus, we focussed on heterologous expression of this interesting oxidoreductase, using the successful *E. coli* expression system in combination with previously for HRP, LiP and VP optimized re-folding and haem insertion conditions [24-26,31,34], to allow further enzyme kinetic and biochemical characterization. After refolding and purification, approximately 7 mg of active Pr-MnP3 was purified, and the refolding efficiency was 6-7% for the recombinant variants, which is similar in level to the yield of *E. coli* expressed HRP, LiP and VP after refolding [24–26]. Molecular size of engineered Pr-MnP3 and its variants as determined by SDS-PAGE and MALDI-TOF-MS analyses was found to be approximately 36 kDa, which is slightly more than the calculated protein molecular mass of respective translated sequences (Appendix: Table S1, Fig. S1).

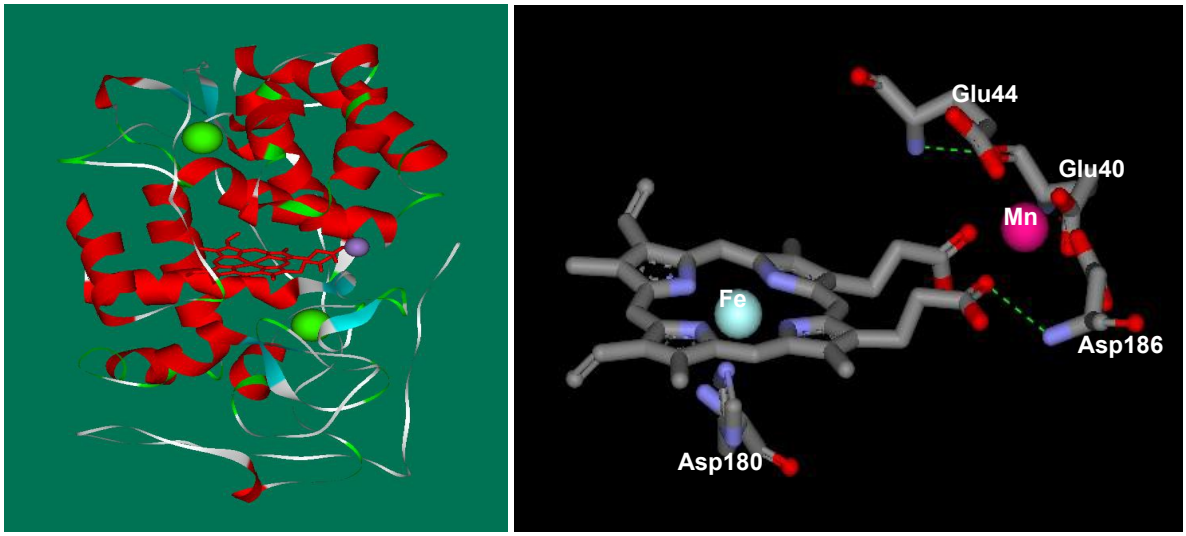

Figure 2. Left: overall fold structure of recombinant Pr-MnP3 enzyme. Haem skeleton is depicted in red, Mn ion sphere in purple, and two Ca ions as green spheres. α-helixes are illustrated in red and β-strands in white. **Right:** manganese-ion binding site in Pr-MnP3. Haem vicinity Asp180 with propionate associated ligand and Mn^{2+} ion (pink sphere) coordinating acidic amino-acid residues (Glu44, Glu40, Asp186) are shown. Haem carbon atom skeleton in grey, nitrogen atoms in blue, oxygen atoms in red.

Protein structurally, Pr-MnP3 represents the short-type of manganese peroxidases (short-MnPs), which are similar in protein fold to class-II LiP and VP crystal structures (Fig. 2), and having a shorter C-terminal tail than is characteristic to the typical long-MnP enzymes such as MnP1 from *Phanerochaete chrysosporium* [1,4,7-9,18,22]. However, the Mn^{2+} ion binding site of MnP structures near the vicinity of one of the haem propionates [22,43] is conserved in Pr-MnP3 [9], which is similar to the observed topology and Mn coordination at this site in long-MnPs and VPs [4,8,9,22,43].

Recently, native fungal class-II atypical short-MnP enzymes with less-conserved Mn-binding sites have been cloned and heterologously expressed [44], and accumulating genomic data pinpoints that these type of atypical short-MnPs are common in Basidiomycota species, owing protein characters of LiP, VP and MnP enzymes, but modulations in their Mn-binding site ligands [4-6,44]. In the atypical short-Ap-MnP1, increase in pH range for Mn^{2+} oxidation was observed [44]. Therefore, a set of site-directed mutants of Pr-MnP3 with modifications at the Mn binding site (Fig. 2) were created (E40H, E44H, E40H+E44H, D186H and D186N). The codon numbering (E40, E44 and D186) corresponds to engineered coding sequence of the recombinant Pr-MnP3 (Fig. 2), being identical to the amino-acid residues of E37, E41 and D183, respectively, which were assigned as the ligands for Mn^{2+} binding in the native enzyme [9]. Moreover, catalytic abilities of engineered Pr-MnP3 were tested in oxidation and conversion of various aromatic substrates including the dye RB5 and several lignin-model compounds, to explore the enzyme's Mn-independent activity and possibility for a second aromatic reducing substrate binding site, as has been identified in a few VP enzymes [4,8,39].

3.2 Characteristics of the Pr-MnP3 Mn-binding site mutants

The UV/visible spectrum (Appendix: Fig. S2) of the recombinant Pr-MnP3 indicates the Soret band maximum at 408 nm, and additional lower absorbance bands at 507 and 641 nm. These spectral characteristics are very similar to those of *P. radiata* MnP2 with 407 nm Soret maximum, and 508 and 640 nm absorbance bands [46], and *P. chrysosporium* MnPH4, with 406 nm Soret maximum, and 502 and 632 nm lower absorbance bands, respectively [12,18]. The R_z values were high for the recombinant Pr-MnP3 (R_z 5.6) and its variants (R_z

4.4-5.2) (Appendix: Table S1), thus confirming success in enzyme re-folding and purification, except for the E40H mutant (R_z 2.1), indicating presence of incorrectly or partially folded and non-haem containing apoproteins in this preparation. The spectral characteristics of recombinant Pr-MnP3 are typical of a hexa-coordinate high spin haem protein, like LiPH8, but clearly distinct from the penta-coordinate classical high spin peroxidases such as HRP [47], and its Mn^{2+} ion coordinating site variants were very similar except for E40H (Appendix: Table S1, Fig. S2), indicating that mutation at the Mn-binding site may cause minimal distortion to the haem environment. A peculiar property of the E40H variant enzyme, however, was protein aggregation, which was not observed in the other Pr-MnP3 variants.

Table 1. Steady-state kinetic data of the recombinant Pr-MnP3 and its Mn-binding site variants

	Mn(II) as the reducing substrate at pH 5.0			ABTS as the reducing substrate at pH 3.0			Molecular size of the enzymes	
Enzyme variants	K_m (mM)	k_{cat} (s^{-1})	k_{cat}/K_m (mM^{-1} s^{-1})	K_m (mM)	k_{cat} (s^{-1})	k_{cat}/K_m (mM^{-1} s^{-1})	Actual mass (Da)	Predicted mass (Da)
Pr-MnP3	0.17±0.01	175 ± 0.3	1029	1.4 ±0.1	912 ± 41	651.4	36065	35704
E40H	11 ±0.4	12 ± 0.2	1.0	0.5 ±0.1	369 ± 13	738	36224	35709
E44H	8.5±0.5	12 ± 0.3	1.5	0.3 ±0.1	491 ± 24	1637	36033	35709
E40H+E44H	20 ±3	1.7 ± 0.1	0.08	4.2 ±0.4	615 ± 28	146.4	36086	35714
D186H	23 ±3	0.84± 0.1	0.04	0.24±0.03	1007 ± 27	4196	36057	35726
D186N	30 ±3	8.0 ± 0.5	0.30	1.3 ±0.1	762 ± 28	586	36051	35703

Steady state kinetic parameters of the recombinant Pr-MnP3 on oxidation of Mn^{2+} (to Mn^{3+}-tartrate complex) indicate that the enzyme is catalytically a manganese-oxidizing peroxidase with a high affinity Mn-binding site (K_m 170 µM) at pH 5.0 (Table 1), and reactivity towards Mn^{2+} was significantly weakened by alteration of the Mn-binding ligands, thereby confirming that the modelled (Fig. 1) and mutated Mn-binding site is the single productive catalytic site for Mn^{2+} oxidation in the enzyme. Moreover, it was noticed that the pH optimum of Mn^{2+} oxidation is at pH 5.0 rather than 4.5, which is the generally used pH in the MnP assays [17].

However, a second reducing substrate binding site cannot be completely ruled out because oxidation of ABTS occurred at low pH (pH 3.0) without addition of Mn^{2+}, and ABTS oxidation was enhanced with mutations at the Mn-binding site towards weaker Mn^{2+}

coordinating non-acidic amino-acid ligands, particularly in the D186H variant (Table 1). In the wild-type native Pr-MnP3 enzyme (Appendix: Table S2), this was previously predicted due to observed slow oxidation of not only ABTS but 2,5-dimethoxyhydroquinone and *o*-dianisidine in the absence of added Mn^{2+} ions. Mn-independent activity of the native enzyme, however noticeable, is less than 12% of the total conversion of dimethoxylated phenols and anisidine (Table 2). It should be noted that no oxidation of veratryl (3,4-dimethoxybenzyl) alcohol was observed by the native enzyme, either in the presence or absence of Mn^{2+} ions (Appendix: Table S2), which is contrary to the slow Mn-independent oxidation ability of VP peroxidases towards veratryl alcohol [1,7,8,39,48], thus confirming the primary role of Pr-MnP3 as a Mn^{2+} oxidizing enzyme.

Table 2. Manganese dependence of substrate oxidation by native wild-type Pr-MnP3. Enzyme activities were measured in the absence and presence of 0.5 mM Mn^{2+} at pH 4.5 with 0.1 mM H_2O_2 and 7.5-20 μM of each substrate. Product formation was followed at specific wavelengths [39].

Reducing substrate	λ (nm)	(+Mn^{2+}) ΔA min^{-1}	(- Mn^{2+}) ΔA min^{-1}	Mn-independent activity (%)
ABTS	420	22.56	1.51	6.7
o-Dianisidine (3,3'-dimethoxybenzidine)	460	4.03	0.29	7.2
2,5-Dimethoxyhydroquinone (2,5-dimethoxybenzene-1,4-diol)	450	5.30	0.61	11.6
2,6-Dimethoxyphenol	469	10.21	0.032	0.3
Veratryl alcohol	310	n.o.*	0.0066	n.d. **

*not oxidised; **not determined because all activity was Mn-independent

3.3 Dye-decolorizing activity

With 10 μM RB5 as substrate at pH 3.0 and 25 °C (0.2 ng of each enzyme), it was noticed that the recombinant and engineered peroxidases were able to bleach the blue coloured dye compound (Fig. 3 A,B). This is surprising, since RB5 has been used as a specific substrate for the DyP activity, and detection of DyP enzymes in fungal culture fluids is based on the bleaching assay [40]. Our results indicate that oxidation and bleaching of RB5 is more like a general ability for the divergent fungal secreted haem-including peroxidases irrespective of the peroxidase class or superfamily [1]. One exception was the engineered

CiP-LiP, which showed no bleaching in the course of the 20 min reaction incubation, which is similar to the influence of the wild-type LiP (Fig. 3 A,B).

Fastest bleaching was catalysed by the recombinant PcLiPH8 and in particular, its E250Q+E168Q double mutant variant [31], demonstrating a rapid bleaching phase within the first two minutes (Fig. 3 A,B). The rapid phase was followed by a slower second bleaching phase, which was continuing over five minutes. It should be noted that also the recombinant PrMnP3 was able to cause constant bleaching of RB5 under these conditions, and with no addition of Mn^{2+} ions, which is confirming the existence of an additional reducing substrate binding site (see chapter 3.2), most likely at the protein surface near the haem channel, likewise was modelled in a few *Pleurotus* VP enzymes [4,8,48].

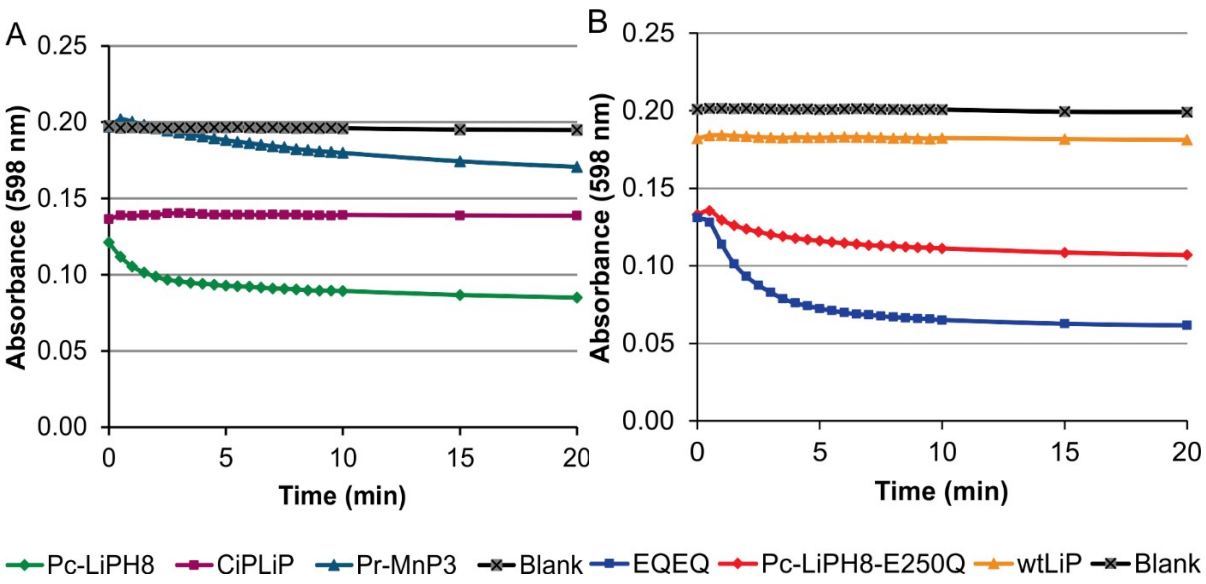

Figure 3 A, B. De-colorizing of Reactive blue 5 (RB5) by the *E. coli* produced recombinant LiP, CiP-LiP and Pr-MnP3 variant enzymes detected as decrease in absorbance at 598 nm. **(A)** Enzymes Pc-LiPH8, CiP-LiP and the engineered Pr-MnP3. **(B)** Pc-LiPH8 variants E250Q and E250Q+E168Q (EQEQ), and purified natural wild-type Pc-LiPH8 (wtLiP). Blank, reaction without enzyme. Reactions were started with addition of H_2O_2.

3.4 Oxidation and conversion of lignin-like model compounds

Upon comparison of the set of recombinant and engineered fungal class-II heme-including peroxidases, the highest product formation reaction rates (the highest initial k value was ca 1 µkat/µl of enzyme) were achieved for the engineered Pc-LiPH8 with veratryl

alcohol as the reducing substrate (Table 3, Fig. 4). With the two non-phenolic model dimers adlerol (β-O-4 non-phenolic arylglycerol-aryl ether, a lignin model compound) and *p*-adlerol (atypical model compound with the B-ring methoxyl in 4-position) (Fig. 2), the formation of veratraldehyde - as the product of C_α–C_β covalent bond cleavage of the propionate side chain - was much slower for the Pc-LiPH8 enzyme (0.36 and 0.25 μkat/μl, respectively), and resulting with less than half of the maximal product conversion rate reached with veratryl alcohol. These values are comparable to the initial rates of veratraldehyde formation obtained for the adlerol dimer with native fungal secreted and purified LiPs, namely LiPH8 of *P. chrysosporium* [36,49] and LiP3 of *P. radiata* [32,50].

For the lignin-peroxidase engineered double mutant Pc-LiPH8 E250Q+E168Q (hereafter designated EQEQ), the rates for veratraldehyde formation from veratryl alcohol and the non-phenolic adlerol β-O-4 dimer were, however, only 12% and 15% of the values obtained for the non-mutated Pc-LiPH8, and with engineered CiP-LiP, only ca 1% of the Pc-LiPH8 maximal efficiency of veratraldehyde formation was observed (Table 3, Fig. 5). These results clearly support the previous studies on LiP structure-function of the enzyme surface Trp-radical site and its acidity both creating the preferred oxidation site for lignin-like high-redox potential aromatic compounds, and initiation of the long-range electron-transfer to haem [25,31,34,51]. The surface oxidation site at Trp-171 is the initiation site of long-range electron-transfer in LiP (Pc-LiPH8) and *P. eryngii* VP [8,31,34,51], and was engineered to CiP (Trp-introduced CiP-LiP) [31]. Recombinant CiP, on the contrary, could catalyze only diminutive oxidation of veratryl alcohol or the dimeric non-phenolic model compounds (Tables 3,4, Figs. 4,5), which is in line of its considered function as a low-redox potential class-II peroxidase [1,8].

Accordingly, ca 60% of veratryl alcohol (3,4-dimethoxybenzyl alcohol) was oxidized and converted by Pc-LiPH8 to mostly veratraldehyde during the overnight reactions (Figs. 6, 7), as detected by HPLC-DAD and LC-MS. Formation of veratraldehyde is evidence for cleavage of the lignin moiety propane backbone carbon-carbon C_α–C_β linkage [32,50]. Of the dimeric lignin model compounds, the *p*-adlerol dimer was more preferred as the reducing substrate for Pc-LiPH8 than the adlerol dimer in the overnight experiments (Fig. 4), which was, however, not so obvious in the determined initial product formation reaction rates (Table 3) or in the amount of veratraldehyde formed from this substrate (Fig. 7).

Table 3. Calculated rates for veratraldehyde formation at 310 nm, kinetic traces obtained with the *E. coli* produced class-II peroxidases.

	Aldehyde formation /oxidation rate at 310 nm (k value) (µkat/µl)					
Reducing substrate	Pc-LiPH8	Pc-LiPH8-EQEQ	CiP-LiP	CiP	Pr-MnP3	No enzyme
Veratryl alcohol	1.0753	0.1290	0.0097	0.0004	0.0000	0.0000
Adlerol dimer	0.3629	0.0538	0.0043	0.0012	0.0000	0.0000
Para-adlerol	0.2477	0.0538	0.0108	0.0017	0.0000	0.0000
Erol dimer	0.0205	0.0054	0.0142	0.0067	0.0002	0.0000

Table 4. Ratio of (veratraldehyde formation rate)/(respective rate obtained with recombinant Pc-LiPH8) at 310 nm with different *E. coli* produced class-II peroxidases.

	Ratio of aldehyde formation at 310 nm/Pc-LiPH8 conversion rate			
Reducing substrate	LiPH8-EQEQ	CiP-LiP	CiP	Pr-MnP3
Veratryl alcohol	0.120	0.009	0.000	0.000
Adlerol dimer	0.148	0.012	0.003	0.000
Para-adlerol	0.217	0.043	0.007	0.000
Erol dimer	0.263	0.693	0.328	0.009

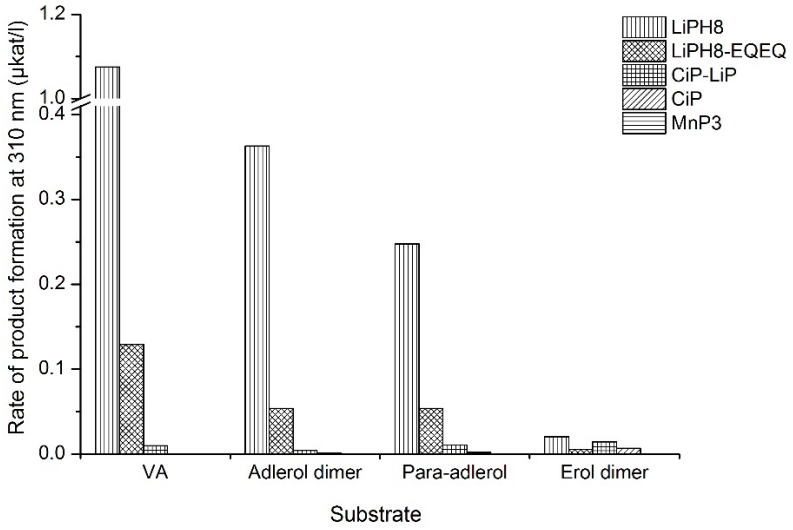

Figure 4. Steady-state kinetic initial rates for product formation (A_{310nm} increase) from lignin-like compounds (see Fig. 2) with *E. coli* produced class-II peroxidases. MnP3, Pr-MnP3 of this study. VA, veratryl alcohol.

Figure 5. Enzyme catalytic efficiency for oxidation and conversion of each substrate (A_{310nm} increase), in comparison to the conversion rate of Pc-LiPH8 recombinant enzyme. VA, veratryl alcohol. For the substrate compound, see Fig. 2.

On the contrary to the specificity of recombinant LiP peroxidases to oxidize and convert the non-phenolic β-O-4 compounds adlerol and *p*-adlerol, oxidation of the phenolic "erol" β–O-4 dimer occurred to some extent with all the engineered class-II peroxidases tested (Table 3, Fig. 5). As observed before (Lundell T, unpublished results) the phenolic β-O-4 dimer erol may act as a reducing substrate for native LiP enzymes. In this study, a slow

trace of a potential benzylic aldehyde formation was observed with all tested recombinant enzymes (0.02 µkat/µl for Pc-LiPH8). If this phenolic β-O-4 dimer would be susceptible to the C_α–C_β propane-chain bond cleavage, the expected product would be vanillin (4-hydroxy-3-methoxybenzaldehyde). However, vanillin was not identified as product by LC-MS and thereby, no product formation rate could be calculated. Nevertheless, it is expected that several end-products are formed from this phenolic dimer lignin-model compound, most likely after oxidation to a reactive phenoxy radical [52].

The Pc-LiPH8 EQEQ double mutant was more efficient in oxidation of the *p*-adlerol and the phenolic erol dimer (22% and 26 %, respectively) than with the monomer veratryl alcohol or the non-phenolic dimer adlerol (Table 4, Fig. 5). The same tendency is seen with the engineered CiP-LiP (Fig. 5), which may reflect that decrease in acidity at the LiP-Trp radical site may in turn promote affinity to phenolic lignin-like compounds. Surprisingly, the engineered CiP-LiP enzyme demonstrated about 70% of the Pc-LiPH8 activity in the oxidation of the phenolic dimer, which was even better than obtained with recombinant CiP (about 33% efficiency) (Fig. 5). These data may, however, also indicate an additional substrate binding and enzyme activation site, which is different from the LiP-Trp171 site, for the phenolic substrate compounds; the additional substrate site may be more near to the distal side of the haem, similar to what is proposed for native *C. cinerea* CiP and a few *Pleurotus* VP peroxidases [1,4,8,45].

In the overnight conversion reactions it was noticed that more veratraldehyde was formed from *para*-adlerol with the LiP mutants (single and double mutants) and with engineered CiP-LiP than the recombinant Pc-LiPH8 (Table 4, Fig. 7), which does not coincide with the initial rate of veratraldehyde formation with the LiP-variants (Table 3). With *para*-adlerol as substrate, in addition to veratraldehyde also additional degradation products were observed in the HPLC traces. These may resulting from the β-O-4 dimer B-ring after the propane chain C_α–C_β bond or ether bond cleavage [32,50,53], the latter of which being chemically more preferred for the *p*-methoxyl substituted dimer molecule (*para*-adlerol) than the B-ring 2-methoxyl substituted adlerol dimer. Additionally noticeable in the overnight conversion reactions is the about 80% conversion of the phenolic erol dimer, which occurred with all the recombinant class-II peroxidases tested except with Pr-MnP3, and may be due to deficiency of Mn^{2+} ions.

Our results with the erol dimer also demonstrate that LiP peroxidases are functional in oxidation and conversion of dimeric phenolic compounds, which is in contrast to recent findings on inactivation of recombinant (*E. coli* produced) Pc-LiPH8 by similar phenolic lignin-like substrate molecules [54]. This discrepancy in results with similar substrates and similar enzymes may be a consequence of differences in reactions conditions and time course followed for the substrate conversion – in our case being fundamentally longer, thus allowing subsequent reactions for the initial radicals formed by enzyme-initiated oxidation (electron withdrawing) of the phenolic substrate molecules.

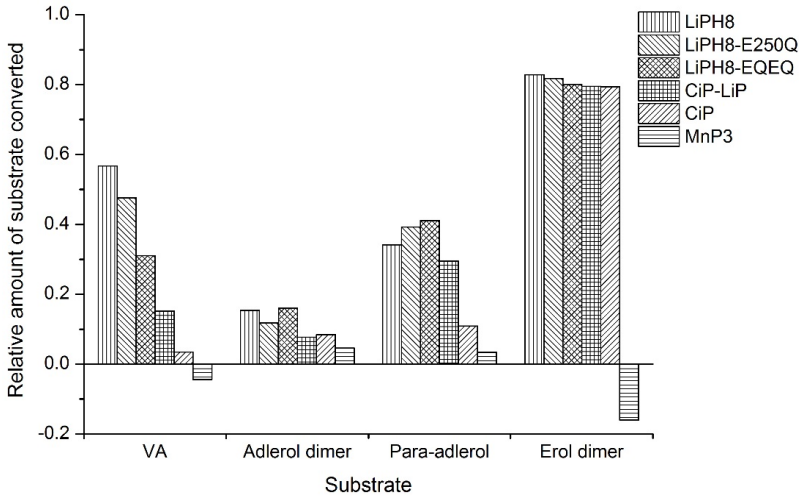

Figure 6. Conversion of the reducing lignin-like substrates (VA, veratryl alcohol) in overnight reactions. One µl of enzyme was added in 1 ml reaction volume, pH 3.0, containing 0.2 mM of each substrate, and the reactions were initiated with 0.2 mM H_2O_2. Each column corresponds the relative amount of substrate detected by HPLC-DAD and confirmed by MS.

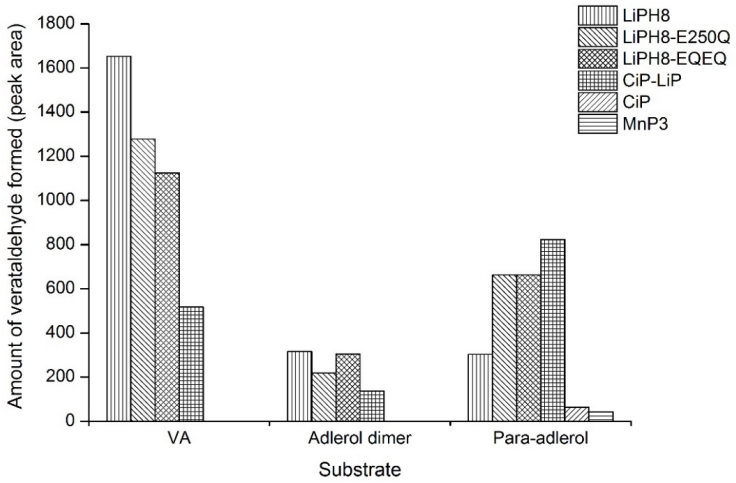

Figure 7. Formation of veratraldehyde (2) from veratryl alcohol (VA, 1) and the lignin-like, non-phenolic dimers adlerol (4) and *para*-adlerol (5), as detected by HPLC analysis. Compound structures, see Fig. 1.

Heterologous expression of class-II fungal peroxidases has allowed recently a few experiments where engineered enzymes have been adopted for bio-conversions. Relation to the reported engineering of a long-MnP class-II peroxidase (from *Ceriporiopsis subvermispora*) to a more VP-like enzyme by introducing a surface oxidation Trp-site [45] showed enzyme stability at very acidic pH conditions, and ability to oxidize and convert by C_α-C_β bond cleavage of a related lignin-like non-phenolic model dimer compound. In addition, trials have been taken for improvement of H_2O_2 stability in class-II peroxidases [55]. It is evident that site-directed mutagenesis allows these specific modifications, and other alterations for improvement of enzyme properties. On the contrary to findings on the instability or catalytic inefficiency of fungal lignin peroxidases in the oxidation of phenolic substrates [54], our results pinpoint quite notable oxidative (and C_α-C_β bond cleaving) activity of Pc-LiPH8 towards the phenolic β-O-4 lignin-like dimer (guaiacylglycerol-β-guaiacyl ether, erol). In addition, no veratryl alcohol was added in the reactions, thereby also questioning the requirement of veratryl alcohol and its cation radical acting as charge transfer mediator for LiP and a necessary protectant for the enzyme [56] in reactions with lignin-like phenolic compounds.

3.5 Conclusions

We report on successful expression of short-manganese peroxidase Pr-MnP3 and its variants using *E. coli* expression system, and comparison of various class-II engineered peroxidases in oxidation and conversion of aromatic compounds. Recombinant Pc-LiPH8 and its variants demonstrated oxidation of veratryl alcohol and non-phenolic (methoxylated) lignin-like compounds (adlerol and *para*-adlerol), and catalysed cleavage of their propane backbone C_α–C_β linkages leading to formation of veratraldehyde. All LiP variants, CiP-LiP and recombinant CiP were also able to efficiently oxidize the phenolic aryl ether dimeric lignin model compound (erol). Mutations at the Pr-MnP3 manganese-binding site resulted with slower oxidation rates and lower affinity to Mn^{2+} ions thus pointing to catalytic characteristics of a typical manganese-oxidizing peroxidase. However, without addition of Mn^{2+} ions, Pr-MnP3 was able to decolorize the anthraquinone dye Reactive Blue 5, which was similar to the bleaching activity of Pc-LiPH8 and its variants. Our results demonstrate

suitability of the recombinant and engineered fungal class-II short-MnP and LiP peroxidases for dye-decolorizing, and applicability of the LiP variants for degradation of non-phenolic and phenolic lignin-like compounds. Recent advances in enzyme engineering, together with our findings, are promising indications of the adoptability of fungal class-II peroxidases as biocatalysts for activation and modification of lignins and lignin-derived chemicals.

Competing interests. The authors declare that they have no competing interests.

Author's contribution. TL, ATS and WD conceived the study. ATS, TL, KH, PN and WD designed the experiments. EB, WD, UFU, JR, JK, MH, TL and MW performed the experiments. TL, WD, ATS, JR, PN and MW analyzed the data. TL, WD, JK, PN, and KH drafted and revised the paper. TL, KH, JK, PN, JR, MW, MH and ATS read and approved the manuscript.

List of Abbreviations

ABTS, 2,2'-azino-bis(3-ethylbenz-thiazoline-6-sulphonic acid); CcP, cytochrome *c*-peroxidase; CiP, *Coprinopsis* (*Coprinus*) peroxidases; CiP-LiP, LiP-like engineered CiP; DAD, diode-array detection; DyP, dye-decolorizing peroxidase; HPLC, high-performance liquid chromatography; HRP, horse radish peroxidase; LC-MS, liquid-chromatography mass-detection analysis; LiP, lignin peroxidase; MALDI-TOF-MS, matrix assisted laser desorption ionization-time of flight-mass spectral analysis; Mn, manganese; MnP, manganese peroxidase; RB5, Reactive Blue 5; R_z, Reinheitszahl; VP, versatile peroxidase; wt, wild-type;

Acknowledgements

The study was supported by the Academy of Finland research projects Ox-Red (#138331) and Luomukat (#133022), and the European Union project BIORENEW (NMP2-CT-2006-026456). The authors thank Dr Jussi Sipilä from the Department of Chemistry, University of Helsinki, Finland, for providing the lignin model compounds.

REFERENCES

[1] Hofrichter M, Ullrich R, Pecyna MJ, Liers C, Lundell T. New and classic families of secreted fungal heme peroxidases. Appl Microbiol Biotechnol 2010; 87: 871–97.

[2] Oliva M, Theiler G, Zamocky M, *et al.* PeroxiBase: a powerful tool to collect and analyse peroxidase sequences from Viridiplantae. J Exp Bot 2009; 60: 453–59.

[3] Welinder K. Plant peroxidases: structure-function relationships In: *Plant peroxidases 1980-1990, Topics and detailed literature on molecular, biochemical and physiological aspects*; Penel C, Gaspar TH, Greppin H, Eds.; University of Geneva: Geneva, 1992; pp. 1-24.

[4] Ruiz-Dueñas FJ, Lundell T, Floudas D, *et al.* Lignin-degrading peroxidases in Polyporales: an evolutionary survey based on 10 sequenced genomes. Mycologia 2013; 105: 1428–44.

[5] Floudas D, Binder M, Riley R, *et al.* The Paleozoic origin of enzymatic lignin decomposition reconstructed from 31 fungal genomes. Science 2012; 336: 1715–19.

[6] Lundell TK, Mäkelä MR, de Vries RP, Hildén KS. Genomics, lifestyles and future prospects of wood-decay and litter-decomposing basidiomycota. In: *Advances in Botanical Research*; Francis, MM Ed.; Academic: London, 2014; Vol. *70,* pp. 329–70.

[7] Martínez AT. Molecular biology and structure-function of lignin-degrading heme peroxidases. Enzyme Microb Technol 2002; 30: 425–44.

[8] Ruiz-Dueñas FJ, Morales M, García E, Miki Y, Martínez MJ, Martínez AT. Substrate oxidation sites in versatile peroxidase and other basidiomycete peroxidases. J Exp Bot 2009; 60: 441–52.

[9] Hildén K, Martinez AT, Hatakka A, Lundell T. The two manganese peroxidases Pr-MnP2 and Pr-MnP3 of *Phlebia radiata*, a lignin-degrading basidiomycete, are phylogenetically and structurally divergent. Fungal Genet Biol 2005; 42: 403–19.

[10] Lundell TK, Mäkelä MR, Hildén K. Lignin-modifying enzymes in filamentous basidiomycetes - ecological, functional and phylogenetic review. J Basic Microbiol 2010; 50: 5–20.

[11] Petersen JFW, Kadziola A, Larsen S. Three-dimensional structure of a recombinant peroxidase from *Coprinus cinereus* at 2.6 Å resolution. FEBS Lett 1994; 339: 291–96.

[12] Glenn JK, Gold MH. Purification and characterization of an extracellular Mn(II)-dependent peroxidase from the lignin-degrading basidiomycete, *Phanerochaete chrysosporium*. Arch Biochem Biophys 1985; 242: 239–41.

[13] Paszczyński A, Huynh V-B, Crawford R. Enzymatic activities of an extracellular, manganese-dependent peroxidase from *Phanerochaete chrysosporium*. FEMS Microbiol Lett 1985; 29: 37–41.

[14] Hatakka A. Lignin-modifying enzymes from selected white-rot fungi: Production and

role in lignin degradation. FEMS Microbiol Rev 1994; 13: 125–35.

[15] Johjima T, Itoh N, Kabuto M, *et al.* Direct interaction of lignin and lignin peroxidase from *Phanerochaete chrysosporium*. Proc Natl Acad Sci U S A 1999; 96: 1989–94.

[16] Hatakka A, Hammel KE. Fungal biodegradation of lignocelluloses. In: *The Mycota: a comprehensive treatise on fungi as experimental systems for basic and applied research*; Esser K, Hofrichter M, Eds.; 2nd ed. Springer: Berlin, Heidelberg, 2010; pp. 319-40.

[17] Wariishi H, Valli K, Gold MH. Manganese(II) oxidation by manganese peroxidase from the basidiomycete *Phanerochaete chrysosporium*. Kinetic mechanism and role of chelators. J Biol Chem 1992; 267: 23688–95.

[18] Gold MH, Youngs HL, Gelpke MD. Manganese peroxidase. Met Ions Biol Syst 2000; 37: 559–86.

[19] Wariishi H, Valli K, Gold MH. In vitro depolymerization of lignin by manganese peroxidase of *Phanerochaete chrysosporium*. Biochem Biophys Res Commun 1991; 176: 269–75.

[20] Glenn JK, Akileswaran L, Gold MH. Mn(II) oxidation is the principal function of the extracellular Mn-peroxidase from *Phanerochaete chrysosporium*. Arch Biochem Biophys 1986; 251: 688–96.

[21] Hofrichter M. Review: lignin conversion by manganese peroxidase (MnP). Enzyme Microb Technol 2002; 30: 454–66.

[22] Sundaramoorthy M, Youngs H, Gold MH, Poulos TL. High-resolution crystal structure of manganese peroxidase: substrate and inhibitor complexes. Biochemistry 2005; 44: 6463–70.

[23] Fishel LA, Villafranca JE, Mauro JM, Kraut J. Yeast cytochrome c peroxidase: mutagenesis and expression in *Escherichia coli* show tryptophan-51 is not the radical site in compound I. Biochemistry 1987; 26: 351–60.

[24] Smith AT, Santama N, Dacey S, *et al.* Expression of a synthetic gene for horseradish peroxidase C in *Escherichia coli* and folding and activation of the recombinant enzyme with Ca^{2+} and heme. J Biol Chem 1990; 265: 13335–43.

[25] Doyle WA, Smith AT. Expression of lignin peroxidase H8 in *Escherichia coli*: folding and activation of the recombinant enzyme with Ca^{2+} and haem. Biochem J 1996; 315: 15–9.

[26] Pérez-Boada M, Doyle WA, Ruiz-Dueñas FJ, Martínez MJ, Martínez AT, Smith AT. Expression of *Pleurotus eryngii* versatile peroxidase in *Escherichia coli* and optimisation of in vitro folding. Enzyme Microb Technol 2002; 30: 518–24.

[27] Whitwam R, Tien M. Heterologous expression and reconstitution of fungal Mn peroxidase. Arch Biochem Biophys 1996; 333: 439–46.

[28] Nakatsubo F, Sato K, Higuchi T. Synthesis of guaiacylglycerol-β-guaiacyl ether. Holzforschung 1975; 29: 165–8.

[29] Smith A, Doyle W. Engineered peroxidases with veratryl alcohol oxidase activity. International Patent WO/2006/114616, PCT/GB2006/001515, 2006.

[30] Smith AT, Ngo E. Novel peroxidases and uses. International Patent WO/2007/020428 PCT/GB2006/003045, 2007.

[31] Smith AT, Doyle W, Dorlet P, Ivancich A. Spectroscopic evidence for an engineered, catalytically active Trp radical that creates the unique reactivity of lignin peroxidase. Proc Natl Acad Sci U.S.A. 2009; 106: 16084–89.

[32] Lundell T, Wever R, Floris R, *et al.* Lignin peroxidase L3 from *Phlebia radiata*. Pre-steady-state and steady-state studies with veratryl alcohol and a non-phenolic lignin model compound 1-(3,4-dimethoxyphenyl)-2-(2-methoxyphenoxy)propane-1,3-diol. Eur J Biochem 1993; 211: 391–402.

[33] Hofrichter M, Lundell T, Hatakka A. Conversion of milled pine wood by manganese peroxidase from *Phlebia radiata*. Appl Environ Microbiol 2001; 67: 4588–93.

[34] Doyle W, Blodig W, Veitch N, Piontek K, Smith A. Two substrate interaction sites in lignin peroxidase revealed by site-directed mutagenesis. Biochemistry 1998; 37: 15097–105.

[35] Ufot UF. Expression and characterisation of a novel manganese peroxidase from *Phlebia radiata*. PhD Thesis, University of Sussex: Brighton, September 2010.

[36] Tien M, Kirk TK. Lignin peroxidase of *Phanerochaete chrysosporium*. Methods Enzymol 1988; 161: 238–49.

[37] Childs BRE, Bardsley WG. The steady-state kinetics of peroxidase with 2,2’-azino-di-(3-ethylbenzthiazoline-6-sulphonic acid) as chromogen. Biochem J 1975; 145: 93–103.

[38] Mäkelä MR, Lundell T, Hatakka A, Hildén K. Effect of copper, nutrient nitrogen, and wood-supplement on the production of lignin-modifying enzymes by the white-rot fungus *Phlebia radiata*. Fungal Biol 2013; 117: 62–70.

[39] Heinfling A, Ruiz-Dueñas FJ, Martínez MJ, Bergbauer M, Szewzyk U, Martínez AT. A study on reducing substrates of manganese-oxidizing peroxidases from *Pleurotus eryngii* and *Bjerkandera adusta*. FEBS Lett 1998; 428: 141–6.

[40] Sugano Y. DyP-type peroxidases comprise a novel heme peroxidase family. Cell Mol Life Sci 2009; 66: 1387–1403.

[41] Moilanen AM, Lundell T, Vares T, Hatakka A. Manganese and malonate are individual regulators for the production of lignin and manganese peroxidase isozymes and in the degradation of lignin by *Phlebia radiata*. Appl Microbiol Biotechnol 1996; 45: 792–9.

[42] Hildén KS, Mäkelä MR, Hakala TK, Hatakka A, Lundell T. Expression on wood, molecular cloning and characterization of three lignin peroxidase (LiP) encoding genes of the white rot fungus *Phlebia radiata*. Curr Genet 2006; 49: 97–105.

[43] Sundaramoorthy M, Kishi K, Gold MH, Poulos TL. Crystal structures of substrate binding site mutants of manganese peroxidase. J Biol Chem 1997; 272: 17574-80.

[44] Hildén K, Mäkelä MR, Steffen KT, *et al.* Biochemical and molecular characterization of an atypical manganese peroxidase of the litter-decomposing fungus *Agrocybe praecox*. Fungal Genet Biol 2014; 72: 131–6.

[45] Fernández-Fueyo E, Ruiz-Dueñas FJ, Martínez AT. Engineering a fungal peroxidase that degrades lignin at very acidic pH. Biotechnol Biofuels 2014; 7: 114.

[46] Karhunen E, Kantelinen A, Niku-Paavola M-L. Mn-dependent peroxidase from the lignin-degrading white rot fungus *Phlebia radiata*. Arch Biochem Biophys 1990; 279: 25–31.

[47] Veitch NC, Smith AT. Horseradish peroxidase. Adv Inorg Chem 2000; 51: 107-62.

[48] Ruiz-Dueñas FJ, Morales M, Mate MJ, *et al.* Site-directed mutagenesis of the catalytic tryptophan environment in *Pleurotus eryngii* versatile peroxidase. Biochemistry 2008; 47: 1685–95.

[49] Gold MH, Kuwahara M, Chiu AA, Glenn JK. Purification and characterization of an extracellular H_2O_2-requiring diarylpropane oxygenase from the white rot basidiomycete, *Phanerochaete chrysosporium*. Arch Biochem Biophys 1984; 234: 353–62.

[50] Lundell T, Schoemaker H, Hatakka A, Brunow G. New mechanism of the C_α-C_β cleavage in nonphenolic arylglycerol β-aryl ether lignin substructures catalyzed by lignin peroxidase. Holzforschung 1993; 47: 219–24.

[51] Blodig W, Smith AT, Doyle WA, Piontek K. Crystal structures of pristine and oxidatively processed lignin peroxidase expressed in *Escherichia coli* and of the W171F variant that eliminates the redox active tryptophan 171. Implications for the reaction mechanism. J Mol Biol 2001; 305: 851–61.

[52] Nousiainen P, Kontro J, Manner H, *et al.* Phenolic mediators boost manganese and versatile peroxidase catalyzed oxidation of lignocellulosic materials. Abstr Pap Am Chem S 2014; 245: 297.

[53] Hammel KE, Kalyanaraman B, Kirk TK. Substrate free radicals are intermediates in ligninase catalysis. Proc Natl Acad Sci U S A 1986; 83: 3708–12.

[54] Pham LTM, Eom M-H, Kim YH. Inactivating effect of phenolic unit structures on the biodegradation of lignin by lignin peroxidase from *Phanerochaete chrysosporium*. Enzyme Microb Technol 2014; 61-62: 48–54.

[55] Bao X, Huang X, Lu X, Li JJ. Improvement of hydrogen peroxide stability of *Pleurotus eryngii* versatile ligninolytic peroxidase by rational protein engineering. Enzyme Microb Technol 2014; 54: 51–8.

[56] Harvey PJ, Schoemaker HE, Palmer JM. Veratryl alcohol as a mediator and the role of radical cations in lignin biodegradation by *Phanerochaete chrysosporium*. FEBS Lett 1986; 195: 242–6.

Appendix. Supplementary data

Supplementary Table 1. Spectroscopic characteristics of the resting state recombinant Pr-MnP3 and its Mn-binding site variants, in comparison to reported features of native fungal MnP and LiP enzymes. Spectra were recorded in 10 mM sodium succinate, pH 6.0. Rz, the ratio of A_{Soret}/A_{280nm} . The ε_{Soret} value is the mean of 3 readings with acceptable standard deviation.

Class-II peroxidase	**Soret** (nm)	**CTI** (nm)	**CTII** (nm)	**ε_{Soret}** ($mM^{-1}\,cm^{-1}$)	**R_Z**
recombinant Pr-MnP3	408	641	507	173 ± 9	5.6
E40H variant	408	629	–	164 ± 17	2.1
E44H variant	408	642	503	160 ± 17	4.5
E40H/E44H variant	408	641	505	169 ± 9	5.2
D186H variant	408	640	506	170 ± 12	4.4
D186N variant	408	640	506	168 ± 6	5.0
native Pr-MnP2 [46]	407	640	508	–	5.0
native Pc-MnP [17,20]	406	632	502	–	4.5
native Pc-LiP [49]	407	632	500	–	5.0

Supplementary Table 2. Steady-state kinetic properties of native wild-type *P. radiata* Pr-MnP3 enzyme with oxidative and reducing substrates determined at pH 4.5 in sodium malonate buffer.

Substrate	K_m (μM)	k_{cat} (s^{-1})
H_2O_2	1.8	23
Mn^{2+} ($MnCl_2$)	30	18
ABTS	400	3.3
o-Dianisidine (3,3'-dimethoxybenzidine, Fast Blue B)	833	n.c.*
2,5-Dimethoxyhydroquinone (2,5-dimethoxybenzene-1,4-diol)	263	2.0
Veratryl alcohol	n.d.**	n.d.**

*not calculated due to high K_m giving V_{max} ~ 0; **not calculated due to too slow reaction rates

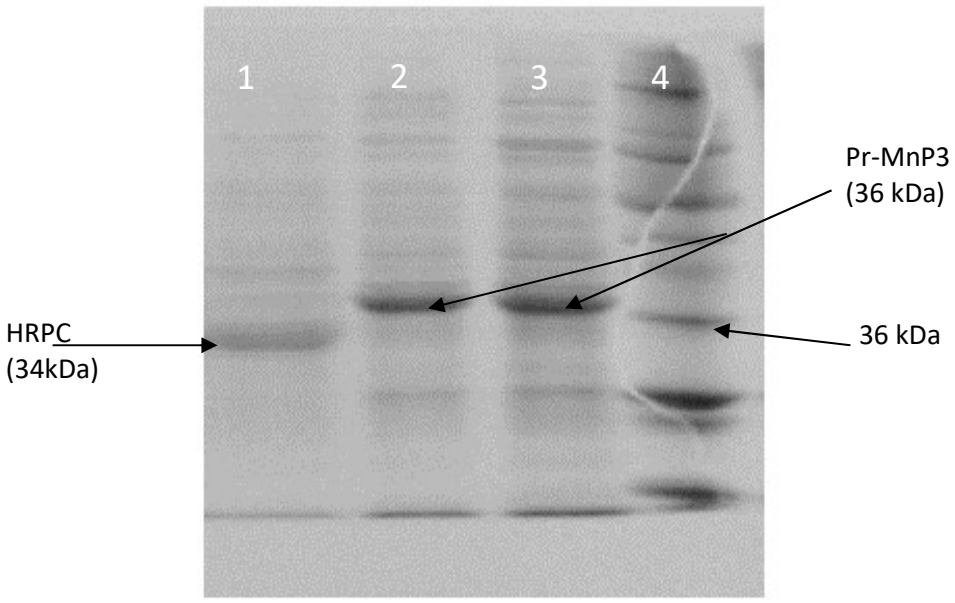

Supplementary Figure S1. SDS-PAGE of insoluble inclusion bodies after small-scale expression of Pr-MnP3. Inclusion body protein pellets were solubilised in 6 M urea and loaded on a 12% resolving SDS-PAGE protein gel. Lane 1 is recombinant horse radish peroxidase isoenzyme C (a class-III peroxidase). Lanes 2 and 3 are proteins from inclusion bodies of the induced *E. coli* cultures. Lane 4 is the protein molecular weight marker (full-range Rainbow, BioRad). Proteins were visualized by Coomassie blue staining and the gel was recorded by digital scanning. As was predicted from the engineered cDNA insert sequence, the size of the recombinant Pr-MnP3 was about 36 kDa.

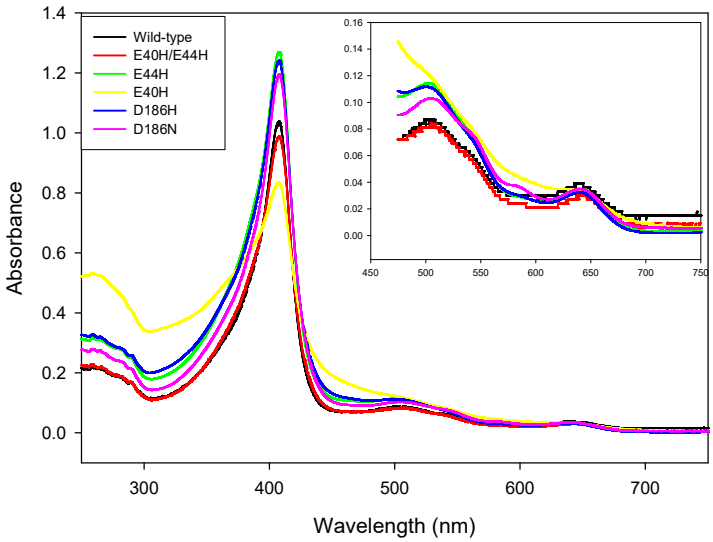

Supplementary Figure S2. Overlay of the resting state UV/Visible absorption spectra for the recombinant Pr-MnP3 and its variants. The spectra were recorded in 10 mM sodium succinate, pH 6.0. (—) wild-type-like enzyme, (—) E40H/E44H, (—) E44H, (—) E40H, (—) D186H and (—) D186N. The insert on the upper right corner is a magnification of the 450 to 750 nm region.